Project Title: **IN-PLANT DEMONSTRATION OF A LOW COST AUTOMATION SYSTEM FOR COAL SPIRALS**

ABSTRACT

Spiral concentrators are widely used in coal preparation plants in Illinois and elsewhere to generally clean the 1 mm x 150 micron particle size fraction. Compound spirals are capable of providing excellent clean coal recovery at reasonably low ash content. The splitter arrangement in a coal spiral controls the cut point between waste and product. It is manually controlled and its position is rarely adjusted once set. As a result, coal spiral yield and product quality suffer when feed quality or feed solid content changes in a coal preparation plant. While such changes are not minute-by-minute; hourly, shift-to-shift, or daily fluctuations are quite common.

The main goal of this project was to demonstrate the functionality of a proprietary automation system for a coal spiral in a real-life plant environment. The automation system was able to adjust the splitter position automatically as and when changes in feed characteristics occurred in an operating coal preparation plant and maintain the desired density cut point at all times. The automation system included two conductivity-based sensors, sensor measurement circuitry, a PIC microcontroller, two tabular solenoids, a DC motor, and a newly designed splitter box. The sensors determine the density gradient in a critical area across the spiral trough. The PIC microcontroller analyzes the density gradient in real time and accordingly actuates the DC motor to move the spiral splitter to the desired location corresponding to the pre-programmed density cut point. Such a spiral automation system not only ensures optimal separation performance from coal spirals, but also helps maximize the overall plant yield for a given product quality by allowing spirals to maintain the same density cut point and thus the same incremental product quality as each of the other cleaning circuits in the coal preparation plant.

The automation system is expected to add an additional cost of $450 to a triple-start set of spirals having the ability to treat nearly 10 tons per hour of raw coal. An expected 2% gain in clean coal yield from this smart spiral circuit would result in additional revenues of $40,000 to $75,000. Clearly, the strong financial gain far outweighs the added cost and justifies quick commercialization of the spiral automation system demonstrated in this project.

EXECUTIVE SUMMARY

Spirals concentrators typically clean 70% of the feed to the fine circuit of a coal preparation plant, which generally amounts to 6 to 8% of the entire run-of-mine coal. They are widely used due to the ease of their operation, their low cost of installation and operation, and their ability to achieve high clean coal yield. However, unlike most other density-based coal cleaning circuits, spiral circuits have no means of being controlled automatically or from a plant control room through a PLC. In fact, the spiral circuit is the only link in the chain of parallel cleaning circuits in a modern day preparation plant which has yet to be automated.

Through two previous ICCI-funded projects, the coal preparation research group at Southern Illinois University (SIU) has successfully developed a proprietary automation system to adjust the splitter position on a full-scale spiral so that a desired density cut point can be achieved by the spiral concentrator even with a fluctuating feed environment. Fluctuating feed conditions commonly encountered in a plant may include changes in feed quality (i.e., coal washability characteristics) or changes in the mass flow of solids to spiral cleaning circuit (i.e., altering the feed solid content). These changes affect spiral cleaning performance and can negatively impact the spiral product if the splitter position remains unaltered. Adjustment of the splitter position is required to maintain a constant density cut point when dealing with these fluctuations. Past studies (Abbott, 1982; Luttrell *et al.*, 2003) indicate that it is essential to maintain the same density cut point for each spiral in a spiral bank to achieve the maximum yield from a spiral circuit. In addition, it is well known that preparation plants operating with multiple parallel cleaning circuits for different size fractions of coal can provide the best possible plant yield for a given product quality only if the incremental product quality achieved in each cleaning circuit can be maintained at the same level, a condition that requires the density cut point for each cleaning circuit to be the same.

The spiral automation system, named SIU's Smart Spiral Component (SSSC), operates on the principle that electrical conductivity of solid particles varies with different types of solid materials. Clean coal particles are known to be generally less conductive than inorganic mineral particles. In fact, a 2nd order polynomial relationship between electrical conductivity and solid density was successfully fitted to experimental data meaning higher density materials resulted in higher electrical conductivity or, in other words, lower electrical resistivity. The SSSC includes two conductivity-based sensors, conductivity measurement circuitry, a PIC microcontroller, two tabular solenoids, a DC motor, and a newly designed splitter box. Each of the two sensors consists of two stainless steel rings placed inside a sampling tube, equipped with a bottom plug controlled by a solenoid. The two sensors are used to establish the density gradient in the critical region (about 7 inch long) across the spiral trough at the discharge end. These sensors measure the conductivity of a settled pack of solids, which is created during the short time period (a couple of minutes) when the bottom of sampling tube is plugged by turning off the solenoid. After the conductivity of the solid pack is measured in each sampling tube, the density gradient between the two measurement points across the spiral trough is established. Based on that measurement and the difference between it and the

previous measurement, a PIC24 microcontroller actuates the DC gear motor to turn clock-wise or counter-clock-wise or to stay at the same position. Both solenoids are then turned on to empty the sampling tubes and complete one control cycle. The control cycle time for the spiral control system in a plant environment is 30 minutes, which can be varied as needed.

The aim of this in-plant study was to demonstrate the functionality of the automation system by operating it on a continuous basis for several months in a real plant environment. The Creek Paum plant, one of Knight Hawk Coal Company's preparation plants operating with two cleaning circuits (i.e., heavy medium cyclone and spiral) served as the host site for this project. One of the four triple-start spirals from the spiral bank was replaced by a new set of smart spirals (triple-start spiral fitted with a SSSC). A new splitter box was designed and fabricated to fit to the discharge end of the triple-start spiral. The electronic printed circuit board (PCB) was designed at SIU, but fabricated and assembled by commercial vendors (Sunstone and Streaming Circuits) to insure structural integrity and reliability in the plant environment. The Creek Paum plant treats coal originating from three different sources with the Hawk Eye Mine being the predominant source. Although the control system was developed with optional switches for three coal types, it was only used for Hawk Eye coal because of the significant number of tests required for calibration and the infrequency with which the other two coals were processed. After the system was calibrated and optimized, a long-term test was conducted over a period of nearly three months to compare the performance of the smart spiral with that of conventional spirals operating in the plant. A total of thirty sets of samples were collected on different operating days for the Hawk Eye coal. An open demonstration of the smart spiral operation, conducted during this long-term test period, was well attended by more than two dozen professionals representing various coal-related organizations in Illinois and beyond.

Comparative clean coal recovery values obtained from smart spirals and conventional spirals, respectively, at a variety of levels of ash rejection were as follow: 91.8% vs. 91.3% at an ash rejection level of 65.7%; 92.3% vs. 89.8% at an ash rejection level of 67.3%; 93.1% vs. 89.9%, at an ash rejection level of 69.7%, and 92.8% vs. 92.7% at an ash rejection level of 71.2%. The improvement in clean coal yield obtained from the smart spiral varied over a wide range, but averaged around 2%. For a triple-start spiral capable of treating nearly 10 tons per hour (tph) of raw coal, this translates to a gain of 0.2 tph of clean coal. Over the course of a year, 800 to 1500 additional tons of clean coal can be sold generating $40,000 to $75,000 of added revenue for each triple-start spiral. Clearly, this strong financial gain far outweighs the added cost of about $450 for the automation system component, justifying quick commercialization of the spiral automation system demonstrated in this project.

OBJECTIVES

The overall goal of this study was to demonstrate the functionality and reliability of SIU's Smart Spiral Component (SSSC) in a real-life plant environment over a long period of time. The SSSC is an automation system for coal spiral concentrators developed at Southern Illinois University with funding in three phases from the Illinois Clean Coal Institute. Specific project objectives were:

➢ Demonstrate the functionality of the automation system on a triple-start spiral operating in a plant environment.
➢ Demonstrate the reliability of the automation system by evaluating its performance over a long period of time (up to 3 months).
➢ Justify the commercial viability of the spiral automation system by conducting an economic analysis.

INTRODUCTION AND BACKGROUND

Spiral concentrators are used in coal preparation plants to clean the nominally 1 mm x 150 micron particle size fraction, which is too fine to be effectively cleaned by a heavy medium cyclone and too coarse for froth flotation cells or flotation columns. The spiral concentrator is a flowing film separator in which the lightest particles move to the outermost section of the spiral profile, whereas the heaviest particles remain in the inner most section. Luttrell *et al*. (2003) explain the misplacement of rock in the clean coal stream due to opposite direction flow patterns in both lower and upper sections of the spiral profile as shown in Figure 1. The optimum position for the splitter is a function of the amount of solids (solid loading) and total slurry (volumetric flow) on the spiral profile, as well as the type of coal (washability characteristics) being treated at a given point in time. Since these three conditions regularly fluctuate in a plant environment due to changes in the coal seam being mined and associated changes in quality and quantity of run-of-mine coal, the splitter position on the spiral trough should also change; however, common practice is to set the splitter position upon installation so that the entire upper section and the upper portion of the lower section report to the clean coal (product) launder, and then leave it alone.
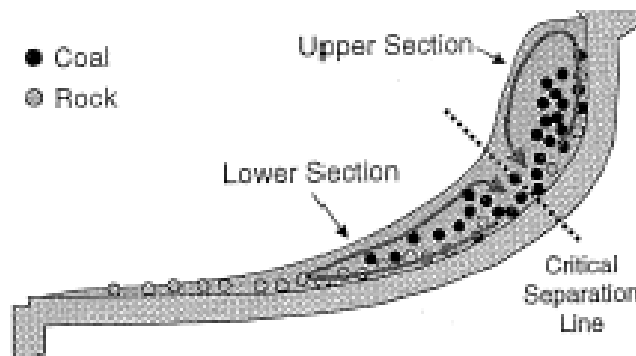

Figure 1: Fluid flow pattern within a spiral cross-section (Luttrell *et al.*, 2003).

4

Previous studies (Mohanty, 2007; Mohanty, 2011) found that the conductivity of a two-phase (solid and liquid) suspension is a function of both solid conductivity and liquid conductivity. After measuring the conductivity of several different types of coal slurry with varying solids content and different types of solid materials in a series of laboratory tests, it was realized that it would be difficult to track solid conductivity and thus specific gravity (SG) of solids in the spiral trough without eliminating, or at least minimizing potential confounding factors such as liquid/solid content. Therefore, it was decided to measure the conductivity of a packed bed of solids in a sensing tube instead of trying to measure the conductivity of the actual solid suspension. As shown in Figure 2, good correlation was found between output voltage and density of solids in a packed-bed sensing tube. Between 1.4 and 1.9 solid mean SG, which adequately covers the density cut point range typically targeted in a coal spiral, this correlation is linear. These test results formed the basis on which a self-emptying tube sensor system was developed to monitor the density gradient across the critical section of the spiral trough.
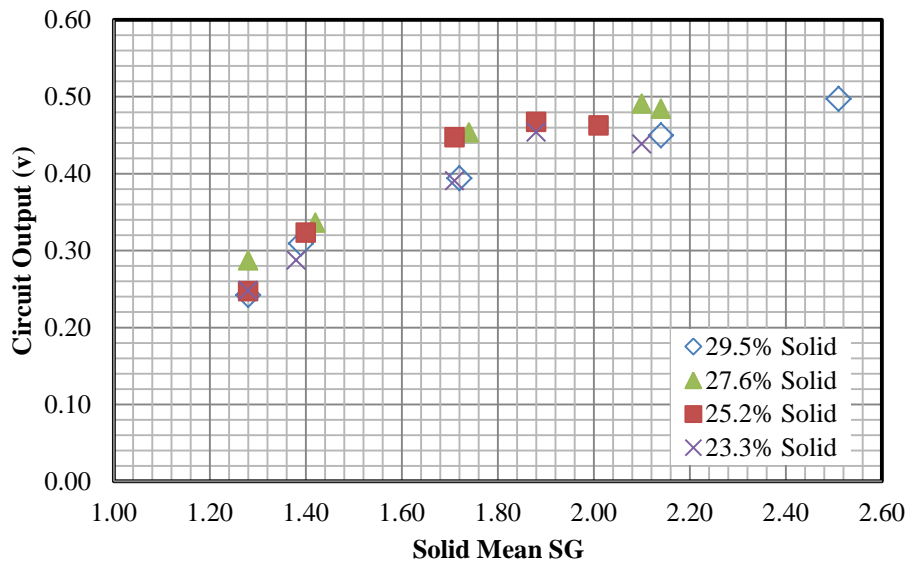

Figure 2: Direct correlation of electrical conductivity and solid density.

The tube sensor developed in Phase 2 of this project (Mohanty, 2011) consists of a Plexiglas tube and two stainless steel rings, as shown in Figure 3. The length and diameter of the tube are critical for solids accumulation and discharge, with optimum length and diameter determined by experimentation. The width of the ring and the separation distance between both rings affect the conductivity constant of the sensor, which determines its level of resolution. A tabular solenoid, as shown in Figure 3, is used to control the sampling process, which consists of three phases: solids accumulation, data recording, and solids discharge. A tabular solenoid is energized to discharge packed solids in about 5-10 seconds, then de-energized for solids to accumulate inside the tube and the sensing circuit to measure and record the conductivity of this packed bed of solids. Based on this measurement and the amount of change from the previous measurement, the PIC microcontroller signals a DC gear motor, which moves the splitter. These components are shown in Figure 4.
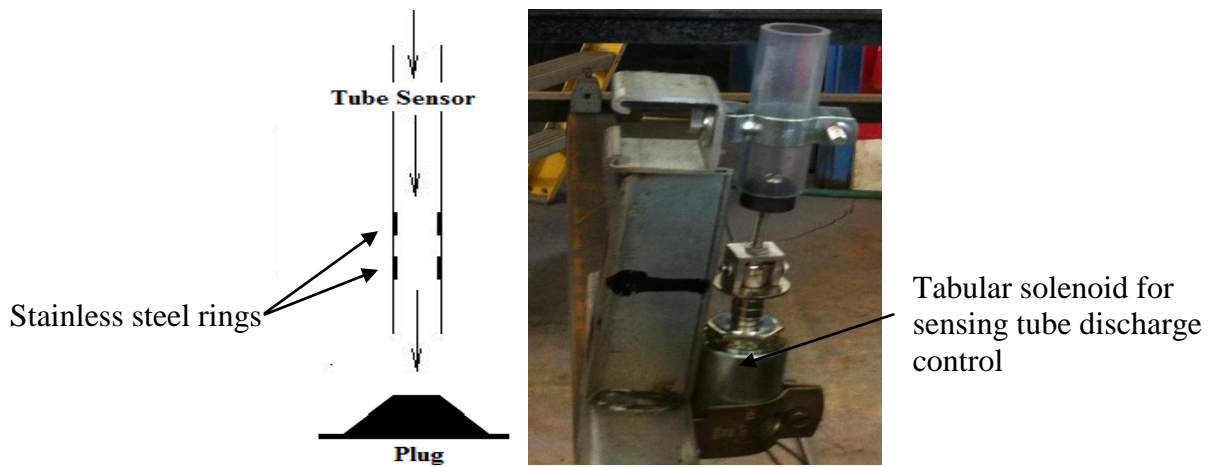
Figure 3: Tube sensor with automated plug driven by tabular solenoid.

Figure 4: Components of the spiral automation system: PIC microcontroller (top left), splitter box (top right), and sensing tubes fed from splitter box (bottom).

EXPERIMENTAL PROCEDURES

Design and Development of In-plant Automation System

Prior to commencing the in-plant demonstration part of this study, a commercial-scale splitter box was designed and fabricated at the Illinois Coal Development Park (ICDP). The splitter box consists of a housing big enough to fit the discharge end of a triple-start spiral, a splitter gate positioned on a gear rack to divide material flowing down the spiral into product and tailings, and two sensing channels to capture a portion of the flow from both upper and lower sections of the spiral trough. Slurry captured in each sensing channel is directed to the tube sensors where the conductivity of settled solids is measured to establish the density gradient between sensing channel locations.

A triple-start spiral with this new splitter box was installed at the Creek Paum coal preparation plant of Knight Hawk Coal Company. Several enhancements were made to the prototype automation system to enable it to maintain its accuracy and endure the harsh preparation plant environment during the extended in-plant demonstration period. Because the power distribution network, AC motors, and other electrical equipment in a coal preparation plant inevitably emit electromagnetic interference (EMI), special attention must be devoted during installation of electronic monitoring systems to make sure that they meet electromagnetic compatibility (EMC) requirements (Kim *et al*., 2006; Muttaqui and Haque, 2008). Although such compliance normally guarantees EMI caused by such systems will not upset the operation of nearby computers or digital control circuits, EMI-induced circuit noise might still be considerable enough to affect and degrade analog signals from the conductivity sensors of the spiral automation system. Various measures were taken during both system development and installation to minimize EMI effects on the spiral automation system. First, proper shielding and grounding were applied for the electronic circuit board and wires connecting the conductivity sensors. Second, an averaging filter was implemented in the microcontroller code to reduce sensor measurement inaccuracies caused by EMI and other noise.

During the in-plant demonstration, the electronic spiral automation system operated in a dusty and humid environment, subject to constant vibration from surrounding equipment. Thus, a highly reliable electronic system design was an essential requirement for the success of the in-plant demonstration. Experience gained from laboratory experiments on the prototype automation system indicated that the power metal-oxide-semiconductor field-effect transistors (MOSFET) used to control circuit relays were prone to failure due to overheating problems. Since these transistors are too small to be used with heat sink devices and the use of a heat exhaust fan system was not practical for this system, the in-plant circuit was modified to reduce MOSFET conducting current by using multiple transistors in parallel to address the overheating problem.

Plant Monitoring and Sampling Methodology

The Creek Paum coal preparation plant of Knight Hawk Coal Company is located north of Murphysboro, IL. Plant capacity is 300 tph and it was designed and installed in 2000

to clean coal from the Creek Paum Mine and other surface mines in the area. The plant cleans the +1 mm size fraction with a single heavy media cyclone circuit and the -1 mm size fraction with four sets of triple-start spirals operating in parallel. These spirals have two outputs: a clean coal product stream and a reject waste stream, which contains both middlings and tailings.

To establish the desired density cut point for the automated spiral, the performance of existing spirals, shown in Figure 5, was evaluated in hourly increments over a period of one week by collecting and analyzing 43 sets of feed, product, and reject samples. Samples were sent to SIU's mineral processing laboratory in Carbondale, IL to determine percent solids and ash content. Coal from three mines – Hawk Eye (HE), Creek Paum North Pit (NPCP), and M21 – were sampled to enable demonstration of the suitability of SIU's spiral automation system to handle changes in plant feed.
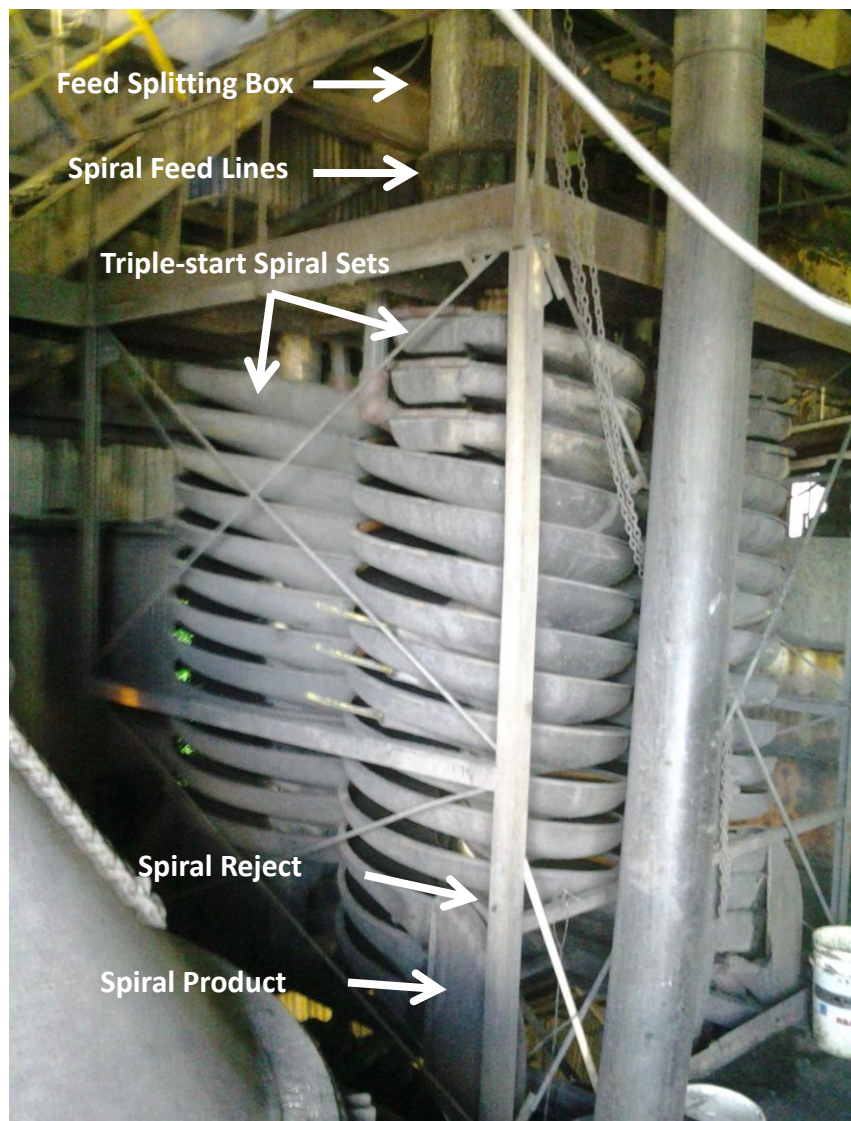

Figure 5: Existing spiral circuit at Knight Hawk Coal Company's Creek Paum plant.

RESULTS AND DISCUSSIONS

Task 1: Characterization of Spiral Feed, Product, and Reject

Sample characterization and spiral performance results for the pre-demonstration baseline sampling regime are shown in Table 1.

Table 1: Baseline sample characterization and spiral performance results.

Coal Type	Test ID	Feed (%)		Product (%)		Tailings (%)		Clean Coal Yield (%)	Combustible Recovery (%)	Ash Rejection (%)	Separation Efficiency (%)
		Ash	Solid	Ash	Solid	Ash	Solid				
Hawk Eye	1	26.7	33.4	11.4	32.4	70.2	54.0	73.9	89.4	68.4	57.8
	2	29.8	34.6	10.4	32.3	64.0	46.9	63.7	81.4	77.8	59.2
	3	24.1	33.0	10.1	29.2	57.2	50.0	70.4	83.3	70.4	53.7
	4	26.6	36.6	11.4	31.9	60.8	48.4	69.3	83.6	70.2	53.8
	5	24.0	35.7	11.4	35.3	62.6	48.2	75.5	88.0	64.0	51.9
	6	20.2	32.1	9.4	29.9	58.1	43.5	77.8	88.3	63.8	52.1
	18	20.3	32.0	10.4	30.5	59.6	45.3	79.9	89.8	59.1	48.9
	19	21.5	31.0	10.3	27.2	64.5	39.0	79.3	90.6	62.0	52.7
	20	25.8	34.8	10.3	30.1	60.8	43.6	69.3	83.8	72.4	56.2
	21	20.8	34.5	9.6	28.8	61.0	42.6	78.1	89.2	64.0	53.2
	22	22.1	33.4	9.6	35.2	57.7	43.1	74.2	86.0	67.5	53.5
	23	23.4	34.2	9.4	30.3	57.5	42.0	71.0	83.9	71.3	55.3
	24	19.8	33.0	9.2	32.4	52.6	41.2	75.5	85.5	65.1	50.6
	25	25.0	32.0	9.6	29.5	57.5	42.2	67.7	81.7	74.1	55.8
	26	21.4	34.0	9.6	34.0	63.2	41.8	78.1	89.7	64.9	54.6
	27	25.3	32.7	10.1	30.9	60.3	44.3	69.7	83.9	72.2	56.0
	28	15.5	32.6	7.8	33.0	52.4	37.7	82.7	90.3	58.5	48.8
	29	25.8	30.8	10.2	27.0	68.4	43.6	73.2	88.6	71.1	59.7
	30	24.9	33.3	9.7	31.7	61.9	43.6	70.9	85.2	72.3	57.6
	31	32.2	34.9	10.8	33.9	67.7	46.2	62.4	82.1	79.1	61.2
	32	32.1	28.8	9.6	6.3	67.1	36.9	60.9	81.1	81.7	62.8
	33	29.7	36.9	12.4	32.0	73.3	50.4	71.5	89.2	70.2	59.4
	34	27.0	41.6	12.4	38.4	63.3	46.7	71.2	85.5	67.5	53.0
	35	33.2	38.6	13.0	36.0	70.5	50.3	64.8	84.4	74.8	59.2
	36	19.9	31.3	8.1	32.0	48.4	36.9	70.6	81.0	71.4	52.4
	41	32.6	45.2	12.5	37.3	73.5	49.7	67.1	87.1	74.2	61.2
	42	27.7	34.7	10.6	29.6	73.1	44.7	72.6	89.8	72.2	62.0
	43	25.3	34.6	12.6	33.9	60.5	38.5	73.4	85.9	63.5	49.5
North Pit Creek Paum	9	39.7	44.0	28.2	37.2	74.8	51.7	75.3	89.7	46.5	36.2
	10	28.4	36.9	13.0	36.0	65.1	45.3	70.5	85.6	67.7	53.3
	11	40.6	40.7	18.0	37.4	70.2	52.6	56.8	78.4	74.7	53.1
	12	42.9	40.7	17.5	34.0	71.7	49.7	53.1	76.7	78.3	55.0
	13	32.2	35.1	15.3	34.8	66.5	47.0	67.1	83.8	68.0	51.7
	14	37.9	42.0	22.5	36.1	70.5	52.2	67.9	84.8	59.7	44.4
	15	31.4	41.9	18.3	35.7	71.0	51.9	75.1	89.5	56.3	45.8
	16	38.6	38.9	17.4	35.1	69.0	50.9	58.9	79.3	73.4	52.7
	17	41.6	37.8	15.7	33.9	72.3	50.6	54.2	78.3	79.5	57.8
	38	37.0	37.7	14.3	33.7	68.8	50.1	58.4	79.5	77.4	56.9
	39	37.2	39.7	19.4	37.0	69.2	51.0	64.3	82.5	66.5	49.0
	40	32.9	43.7	17.9	43.2	67.6	51.4	69.8	85.4	62.0	47.4
M21	7	14.6	23.6	8.1	23.1	41.9	31.0	80.9	87.0	54.8	41.8
	8	15.9	24.8	7.3	22.7	42.3	30.5	75.5	83.2	65.1	48.4
	37	27.9	31.6	11.5	27.1	58.1	38.9	64.9	79.6	73.2	52.8

Results are plotted in Figures 6 and 7 showing variations in feed solids content and feed ash, respectively, versus the following response variables: combustible recovery, clean coal yield, ash rejection, sulfur rejection, and separation efficiency.
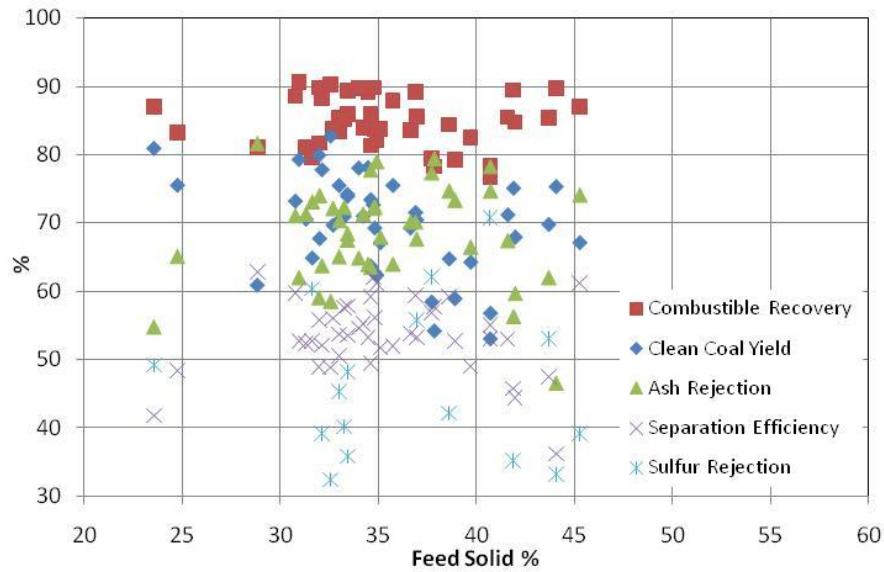

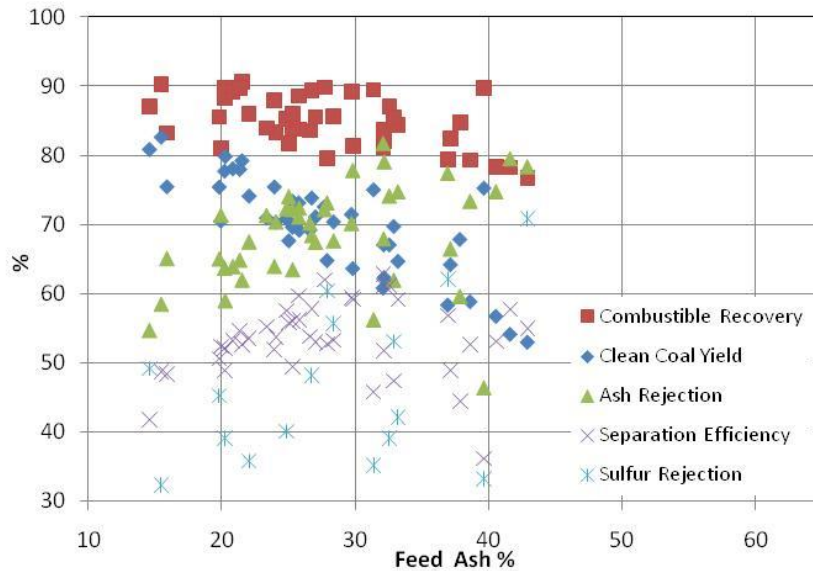Figure 6: Variation in feed solids content versus five response variables.

Figure 7: Variation in feed ash versus five response variables.

As exhibited in Figure 6, solids content of the +100 mesh size fraction of the feed varied from 23.6 to 45.2%, a range of 21.6%. As exhibited in Figure 7, ash content in the feed varied from 14.6 to 42.9%, a range of 28.3%. These figures also show that ash rejection varied from 46.5 to 81.7%, a range of 35.2%; combustible recovery varied from 76.7 to 90.6%, a range of 19.9%; clean coal yield varied from 53.1 to 82.7%, a range of 29.6%; sulfur rejection varied from 29.2 to 70.8%, a range of 41.6%; and separation efficiency

varied from 36.2 to 62.8%, a range of 26.6%. It is believed that variations in feed characteristics cause fluctuations in spiral product and tailings stream qualities, which have not been of interest to most operators; however, these results clearly validate the hypothesis that spiral separation performance is affected by feed characteristics.

Washability tests were done on two feed samples of Hawk Eye coal having the highest and lowest feed ash content to find the optimum density cut point for the spiral circuit. Results, shown in Figure 8, indicate that the ideal SG_{50} for both feed samples is 1.33.
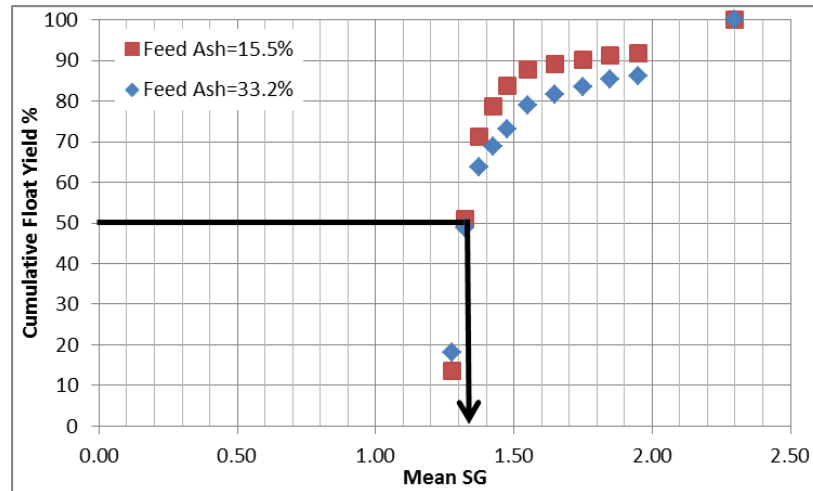
Figure 8: Washability curves for Hawk Eye coal feed samples with highest and lowest ash.

Task 2: Fabrication and Installation of Electronic Circuitry and Splitter Box

Development of Electronic Circuitry for the SSSC

Improvements to the Sensor Measurement Circuit: During the extended field demonstration period, programmability was added to almost every circuit block in the sensor signal chain shown in Figure 9 to make the system more flexible for coping with the challenges of a harsh environment that included large temperature variations, lots of dust and moisture, constant vibration, and interference from other electric-powered devices. In addition, a temperature sensor was added to the system.

Addition of a Temperature Sensor: The temperature sensor enables the system to sense temperature variations, which range from 90°F in summer to 30°F in winter and can affect conductivity readings even when other conditions remain the same. The temperature sensor provides temperature readings to the microcontroller via a serial peripheral interface (SPI) where advanced splitter position control programs can compensate for temperature variation effects.
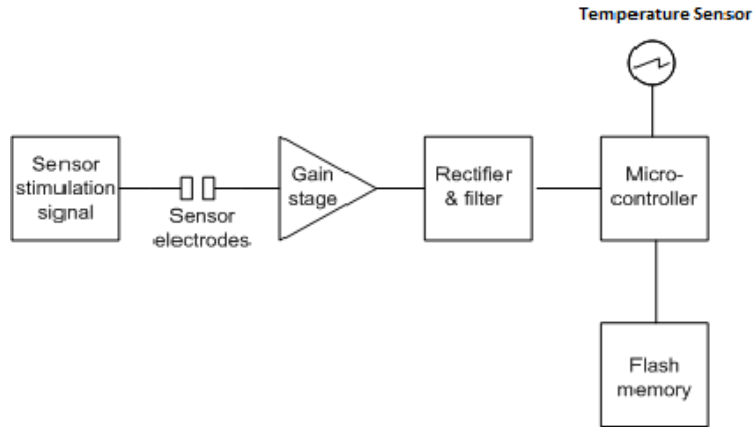
Figure 9: Sensor signal chain in the smart spiral system.

Programmability in Sensor Stimulation Signal: In the first phase design, the sensor stimulation circuit generated a triangular waveform of magnitude (V_A) 125 mV and frequency (*f*) 2 KHz. Results showed this signal to be adequate for laboratory conditions. To prepare the circuit to cope with unexpected and large interference noise during field testing, the sensor stimulation circuit was improved by adding a configuration that can generate an elevated stimulation signal of V_A = 1.15 V and *f* = 250 Hz. The two stimulation signals are compared in Figure 10 with the top left panel showing the original stimulation signal and the bottom left panel showing the elevated stimulation signal. When field test results indicated that the sensor measurement circuit was capable of producing reliable sensor readings with the original stimulation signal, the elevated sensor stimulation signal was not used.

Programmability in the Gain Stage: A larger gain option (X11) was added to the gain stage circuit to amplify small sensor signals. The laboratory circuit provided only one gain option (X1). The new design allows users to select the gain via a jumper. This modification improves the system's capability to handle small sensor signals, which may be encountered during extended periods of operation. During the field test, the gain option was used to help improve measurement accuracy.

Programmability in Rectifier and Filter Circuit: In the first phase design, filter gain (A) was 0.4 and filter bandwidth (f_{BW}) was 2.8 Hz. This small filter gain unnecessarily attenuates sensor output. In the improved design, a second option with A = 1 and f_{BW} = 1.7 Hz was added. Again, users can select the filter configuration by a jumper. The new filter configuration avoids unnecessary signal attenuation and potentially improves circuit noise performance, but it requires a slightly longer settling time due to its narrower bandwidth. Sensor outputs with different filter configurations are compared in Figure 10 with the top right panel showing the sensor output using the original filter and the bottom right panel showing the sensor output using the new filter configuration. Clearly, the new filter configuration leads to a larger magnitude of sensor signal, but settling at a slower pace. With measurement cycle time set at five minutes, this increase in filter settling time is negligible; hence, the narrower filter bandwidth was used during field testing.
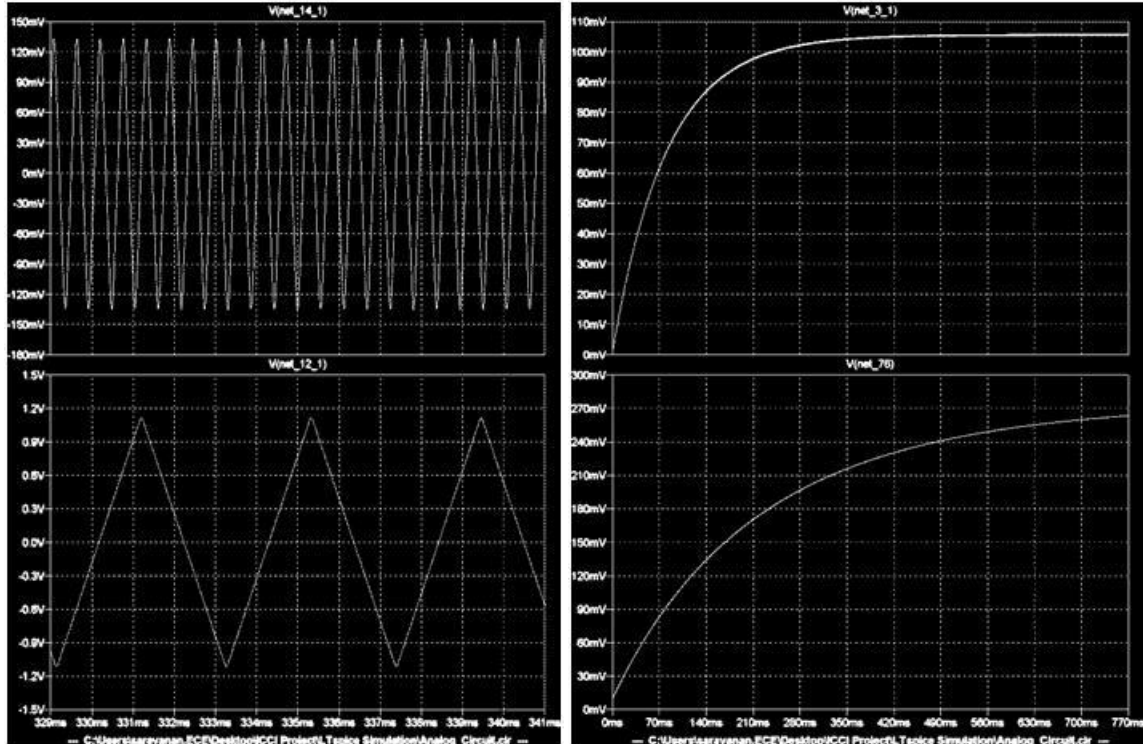
12

Figure 10: Sensor stimulation signals (left) and sensor output with different filters (right).

<u>Investigating Noise Characteristics of Field Data</u>: Sensor signal noise characteristics were investigated in the field using a breadboard prototype circuit where sensor signals were captured by an oscilloscope. A captured sensor signal and its spectrum plot are shown in Figure 11. The ideal sensor signal should be a pure DC signal so the captured signal shows significant noise is present. The fast Fourier transform (FFT) analysis indicates that the majority of the noise is white noise. At 60 Hz frequency, the noise level is slightly elevated to about 20 dB, which is probably due mainly to noise coupled from the power source. Nevertheless, the noise energy is much lower than that of the signal.
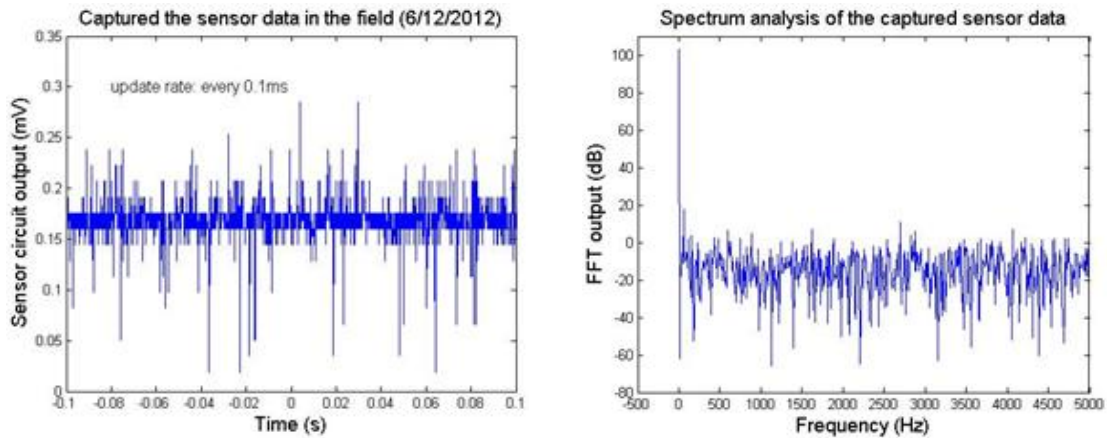
Figure 11: Captured sensor signal (left) and FFT plot of the sensor signal (right).

To cope with the noise, an averaging filtering operation can be performed during the analog-to-digital conversion (ADC) process. For the selected microcontroller (PIC24 family), an averaging-8 operation can be performed during the ADC interrupt subroutine. Figure 12 shows the sensor signal after implementing averaging filtering in the ADC subroutine. The left side of the figure shows the noise level is significantly reduced after one filtering. The right side of the figure shows that additional averaging filters can be implemented after ADC conversion in the microcontroller code. (Note that these data are obtained from Matlab simulation). The investigation suggests that a combination of enhanced current sensor circuit hardware and software averaging filters should be adequate to cope with noise during field application of the SSSC.
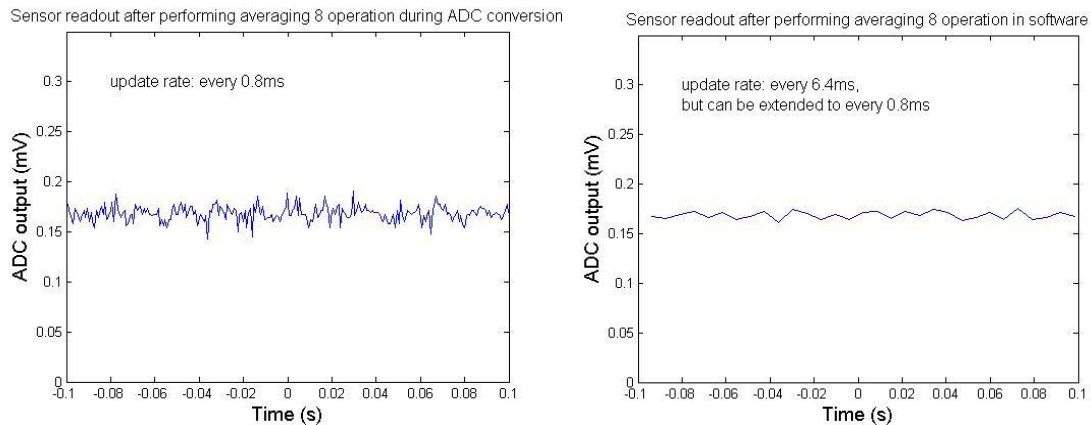
Figure 12: Sensor signal after averaging filter in ADC subroutine (left)
and after additional averaging filter in microcontroller software code (right).

Additional Sensor Circuit Modifications: *Flash Memory*: Extra memory in the form of a 16-Mbit flash cell was added to the sensor circuit for logging system operations, which captures valuable data for system debugging and performance analysis. This flash memory has 4,096 pages and each page contains 528 bytes. It communicates with the microcontroller via a SPI. Log entry data items and their sizes are listed in Table 2. Each entry takes 80 bits (or 10 bytes) and a page can contain 52 data entries leaving eight bytes unused. In the current microcontroller program, the first eight pages are reserved for memory management and other purposes leaving 4,088 pages for storing 212,576 (4,088×52) log entries. With 5-minute cycle times, this amount of memory can record system operations 24 hours per day for almost two years.

Table 2: Data items and sizes in system log entry.

	Data Size (bits)
Conductivity Sensor 1	16
Conductivity Sensor 2	16
Parameter Y for Motor control	16
Coal Type	16
Temperature	16

14

Manual Control for DC Motor and Sensor Tube Solenoids: Occasionally system operators need to manually control the motor that adjusts the splitter position. To accommodate this, two additional switches were added to the motor control circuit as shown in Figure 13. An additional switch was added to allow users to control both sensor tube solenoids without turning on the PCB. This is a two-position switch whose function is described in Table 3. It should be noted that the solenoid control switch should not be in Position 2 if the PCB is on because the manual control will override the PCB control. In the first phase design, it was impossible to isolate the PCB from other high voltage systems including 24V relays, solenoids, and the DC motor. Observed current spikes generated by these high voltage systems often reset the microcontroller and had the potential to damage other circuit components. Adding manual control switches not only provided additional operational flexibility, but also separated the PCB from these high voltage components, thus improving system reliability.
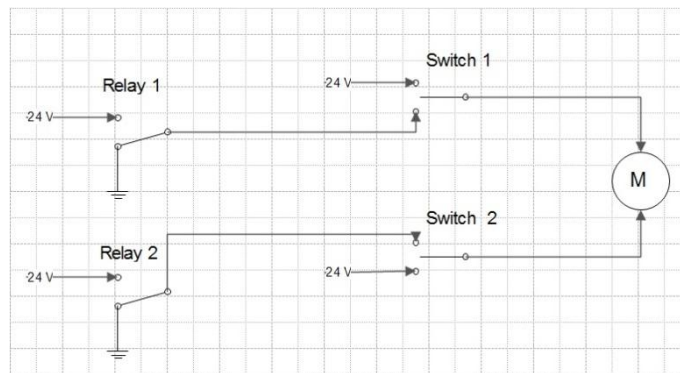

Figure 13: Location of manual motor control switches added to circuit.

Table 3: Functions of the manual solenoid control switch.

PCB State	Switch Position	Function
OFF	1	Solenoids OFF
	2	Solenoids ON
ON	1	PCB control
	2	Solenoids ON

PCB Design: To enable the sensor circuit to reliably survive the harsh plant environment while minimizing sensitivity to the noisy environment, it was assembled on a PCB encapsulated inside a metal box as shown in Figure 14. Caution was taken to avoid cross-talk between noisy digital signals and sensitive analog signals. The metal case was tied to the circuit ground for achieving better EMI shielding. All switches are positioned on the front panel of the instrumentation case. To protect it from water damage, the entire electronic system is covered with plastic material when mounted to the spiral frame during field operations. This arrangement appeared to work well throughout the field demonstration.
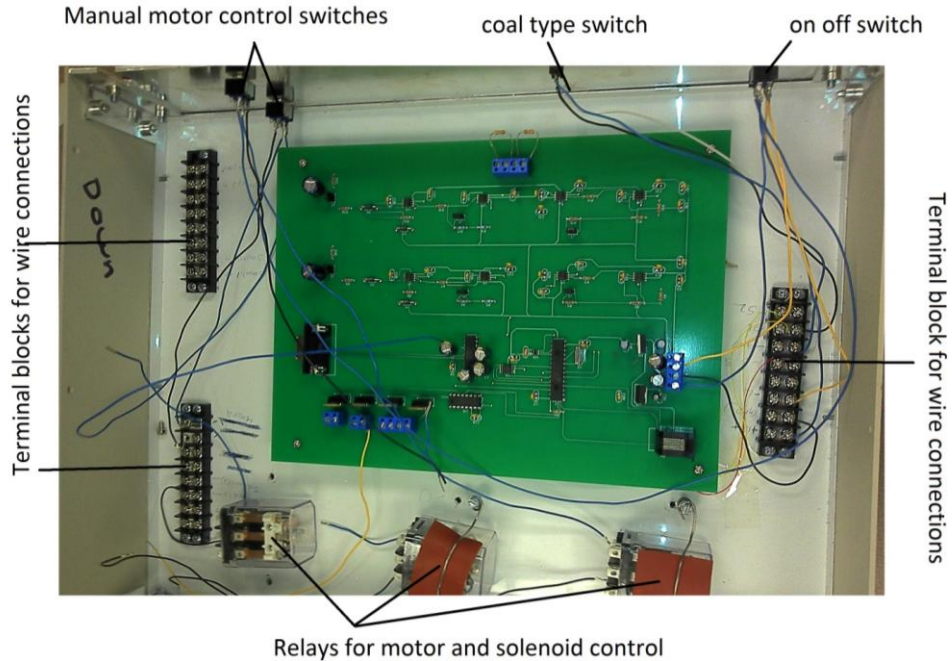
Figure 14: Sensor circuit PCB and switches housed in metal enclosure.

Improvements to the Microcontroller Program: *Communication with Flash Memory*: Initial code was modified so that communication with the 16-Mbit flash memory was possible. The modified code gives users the ability to download data in memory through a universal asynchronous receiver/transmitter (UART) port.

Incorporating Different Coal Types: The modified program code can accommodate three different types of coal. Users can select coal types via two control switches mounted on the front panel of the system. Coal types corresponded to different switch combinations are listed in Table 4.

Table 2: Switch combinations for selecting different coal types.

Switch 1	Switch 2	Operation
OFF (0)	OFF (0)	Memory Read and Erase
OFF (0)	ON (1)	Coal Type 1
ON (1)	OFF (0)	Coal Type 2
ON (1)	ON (1)	Coal Type 3

Other Program Changes: The microcontroller code was modified so that the splitter position would be saved in flash memory when the system was turned off. This allows the system to start with the previous optimal splitter position once it is rebooted. Also, an additional averaging filter was implemented in the microcontroller program code to achieve more stable splitter position control. Finally, the modified program has enhanced flexibility for users to control cycle time and the calculation of new splitter positions.

16

Fabrication of Splitter Box for Triple-start Spiral

A large splitter box was designed and fabricated to fit on the discharge end of a triple-start spiral set (three spiral units on the same foot print) as shown in Figure 15. The splitter box consists of a housing, the splitter gate, a gear rack driven by a DC motor, and two sensing channels. The splitter gate serves all three spiral starts dividing their flow into product and tailings. The automated splitter box installed on a triple-start spiral at the ICDP is shown in Figure 16.
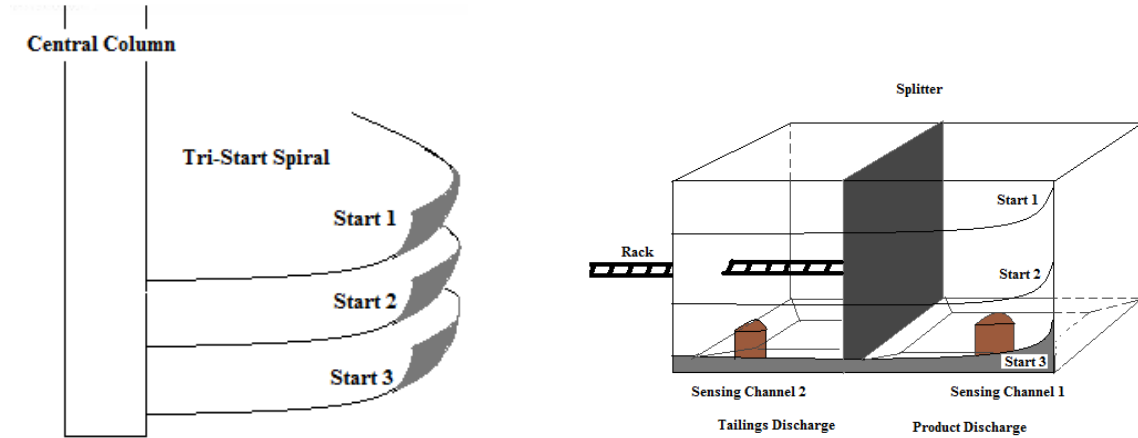
Figure 15: Schematics of triple-start spiral (left) and splitter box (right).
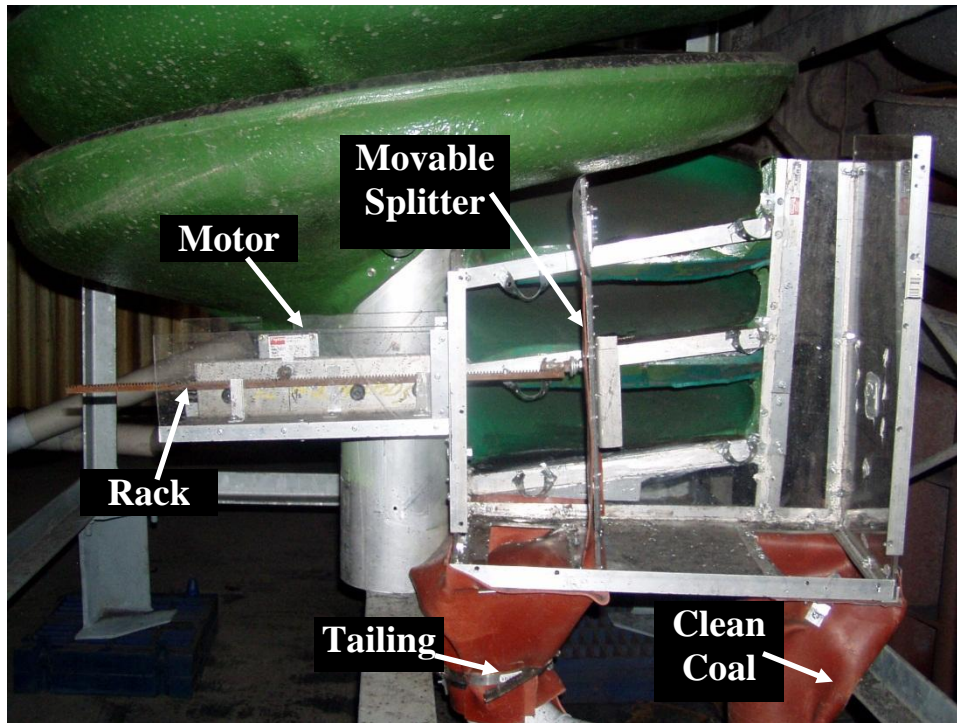
Figure 16: Fabricated splitter box installed on triple-start spiral at ICDP.

In-plant Installation of Triple-start Spiral Equipped with Automated Splitter Box

After assembly was completed at the ICDP, the triple-start spiral with the automated splitter box was installed next to the existing bank of spirals in Knight Hawk Coal Company's Creek Paum preparation plant as shown in Figure 17. Feed piping into the test circuit and discharge piping for clean coal and tailings streams were completed.
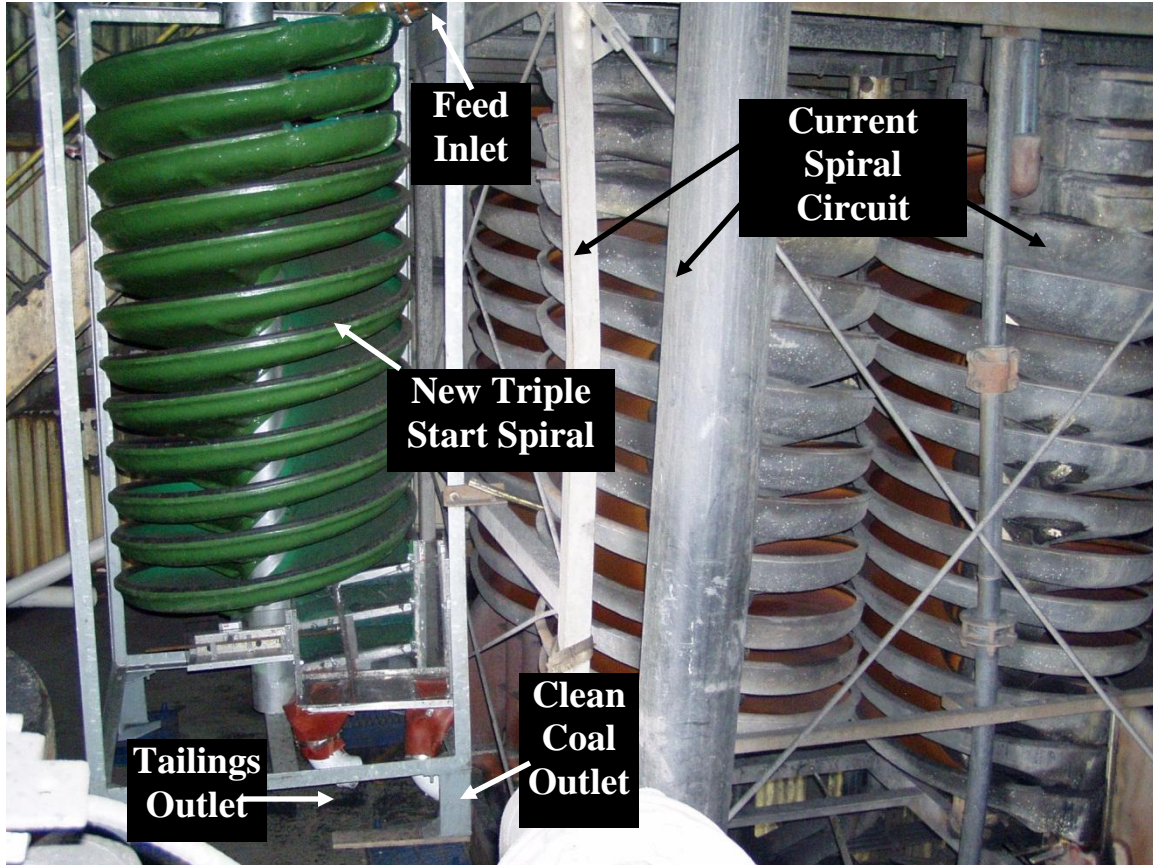

Figure 17: In-plant installation of test spiral circuit equipped with automated splitter box.

Task 3: Initial Testing of the Spiral Automation System

Testing Consistency of Sensor Circuit Readings

Before the automated spiral circuit was installed in the plant, tests were performed in the laboratory on the circuit board and sensors to ensure consistency of readings. Distilled water and salt water (0.1 gram of NaCl in 1000 cc of H_2O) were used in testing sensor tube diameters. Figure 18 shows two 1-inch diameter tubes and two 0.75-inch diameter. Each sensor tube has two 0.25-inch wide rings made of stainless steel located 0.75 inches apart. One of the rings inside each tube is used to send the input voltage to the packed material in the tube and the other ring receives the output voltage based on the conductivity of the packed bed of materials.
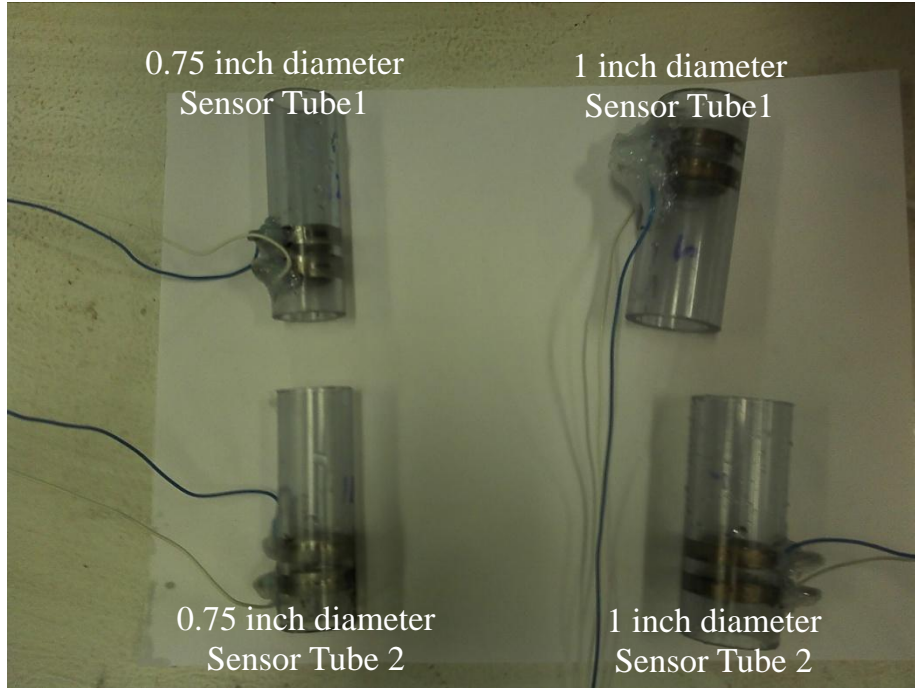
Figure 18: Sensor tubes for testing the effect of diameter.

Table 5 shows results from these tests to check the consistency of readings the sensors and circuit. Channels 1 and 2 represent the two channels of the microcontroller ADC. Each sensor is connected to these channels, which take the analog voltage coming from the sensors and convert it to a digital value. This digital value is then converted into the numbers shown in the table. These numbers represent the conductivity of the packed bed of materials in the sensors; a higher number means higher conductivity. The difference in readings between sensors of the same diameter is due to small variations in the distance between rings inside the sensor tubes and the small variation in readings for the same channel is due to process variation. However, variations are linear so they can be compensated for by calculating the difference between the original readings. Results in Table 5 clearly show consistency indicating that the circuit and sensors were stable.

Table 3: Data from consistency check of sensors and circuit.

Circuit	Readings	1 inch diameter sensors						0.75 inch diameter sensors					
Channel	No.	Distilled Water		Tap Water		Salt Water		Distilled Water		Tap Water		Salt Water	
		Tube 1	Tube 2	Tube 1	Tube 2	Tube 1	Tube 2	Tube 1	Tube 2	Tube 1	Tube 2	Tube 1	Tube 2
Channel-1	1	0	0	41	44	170	176	0	0	33	31	154	144
	2	0	0	41	44	170	176	0	0	33	31	154	144
	3	0	0	41	43	170	176	0	0	33	31	154	144
	4	0	0	41	43	170	175	0	0	33	31	154	144
	5	0	0	42	43	169	175	0	0	33	31	154	144
	6	0	0	41	43	170	175	0	0	33	31	154	144
Channel-2	1	0	0	41	41	169	176	0	0	32	31	153	142
	2	0	0	41	41	169	176	0	0	32	31	153	142
	3	0	0	41	42	169	175	0	0	32	31	153	143
	4	0	0	41	42	169	175	0	0	32	31	153	143
	5	0	0	41	41	169	175	0	0	32	31	153	143
	6	0	0	41	43	169	175	0	0	32	31	153	143

Calibrating Specific Gravity Sensor Circuit

The PCB uses a calibration equation defining the relationship between tailings SG and the difference between the two sensor readings to find the proper position for the splitter. To develop this equation, the splitter box was modified with piping to capture a clean coal and three tailings samples as shown in Figure 19. The clean coal sample collector always fed the clean coal sensor, but the tailings sensor could be fed by any one of the three tailings sample collectors, each positioned in a different location (named 'a,' 'b,' and 'c') along the spiral edge where the splitter moves. After reading the sensor outputs in the field, clean coal and tailings samples were collected and analyzed for SG and ash content in the lab. Results show that clean coal density varies from 1.24 to 1.29 with an average of 1.26 (see Table 6). Knowing this value, the density gradient across the critical separation zone of the spiral trough can be established based on the difference between clean coal and tailings readings.
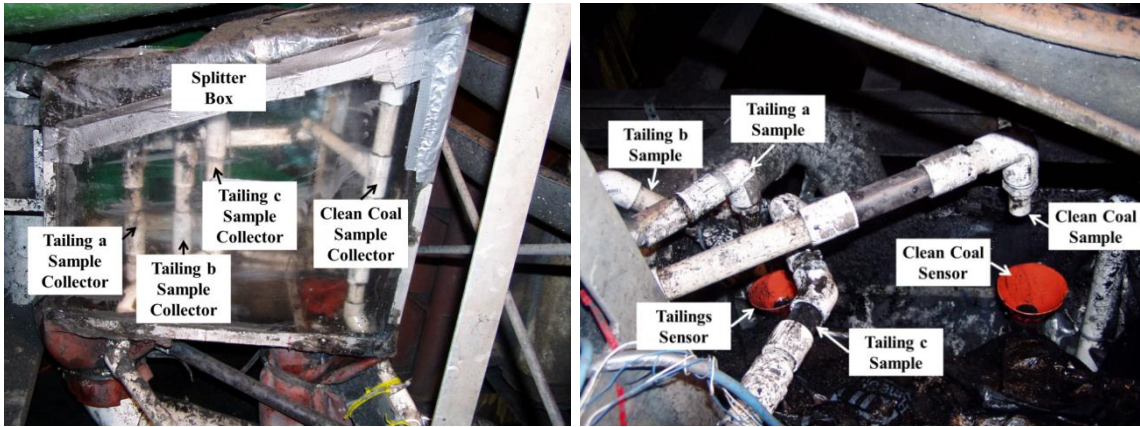

Figure 19: Clean coal and tailings sample collector piping for calibrating sensor circuit.

Table 4: Specific gravity measured at clean coal sensor.

SG Readings at Clean Coal Sensor	1.25	1.26	1.26	1.25
	1.28	1.26	1.26	1.25
	1.24	1.25	1.25	1.25
	1.27	1.29	1.25	1.25
	1.28	1.25	1.24	1.28
Average	1.26			
Standard Deviation	0.02			

Figure 20 shows the relationship between SG and ash content for samples collected from both clean coal and tailings sensors. An equation in the form shown was developed from more than 100 data points to describe ash content (Y) as a function of SG (X). The R^2 value for this equation was 0.99 and parameter coefficients *a*, *b*, and *c* were -97.26, 103.99, and -7.122, respectively.
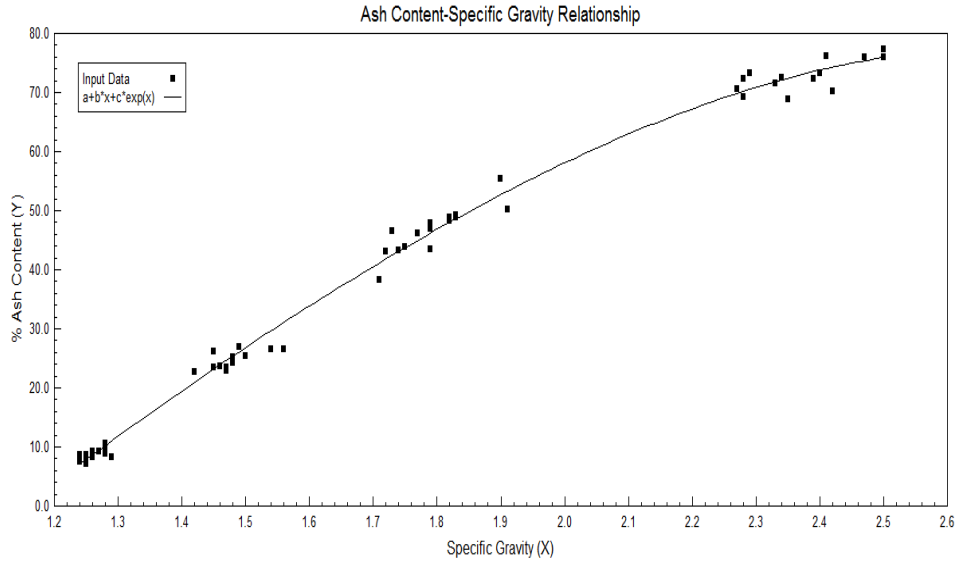
Figure 20: Relationship between specific gravity and ash content for Hawk Eye coal.

With clean coal SG found to be 1.26, it is necessary to determine tailings SG before the splitter position can be adjusted for a desired density cut point. This is done by determining the relationship between the difference in conductivity readings of both clean coal (S2) and tailings (S1) sensors and tailings SG. The calibration line shown in Figure 21 shows this relationship based on data collected in the plant and density measurements for associated samples analyzed in the lab.
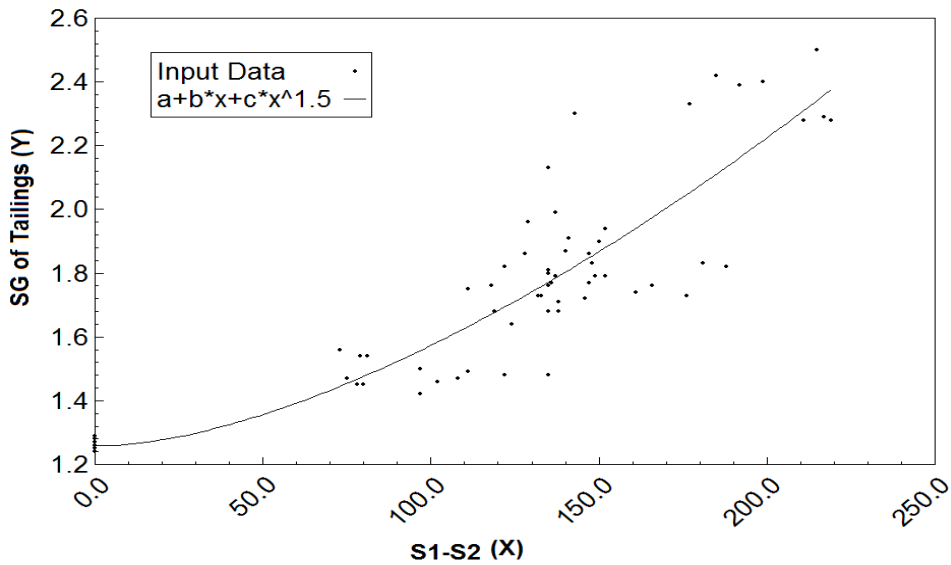
Figure 21: Calibration line showing relationship between difference in sensor readings for clean coal (S2) and tailing (S1) versus tailings SG.

Initially, a linear relationship was assumed based on limited experimental data; however, the curvilinear relationship shown in Figure 21 was found to better fit the relationship after extensive sampling to insure an accurate model equation. Such an effort was

21

undertaken since automatic adjustment of the splitter position would be based on this calibration equation. The R^2 value for this equation was 0.84 and parameter coefficients *a*, *b*, and *c* were 1.26, -9.29E-4, and 4.07E+4, respectively. This equation was programmed into the control system for the field trial with Hawk Eye coal. Similar equations for the other two coals could not be developed due to lack of sufficient data.

Coupling Tailings Sensor Output to Splitter Positioning Mechanism

During testing to determine the calibration equation, it was observed that data variation increased as tailings SG increased. This is shown in Figure 22 where it can be seen that when tailings SG is between 2.25 and 2.50, the difference in sensor readings (S1-S2) varies from 100 to 235; however, when tailings SG is between 1.40 and 1.55, S1-S2 only varies from 75 to 135. Thus, it can be concluded that the accuracy of sensor readings decreases with increase in tailings SG.
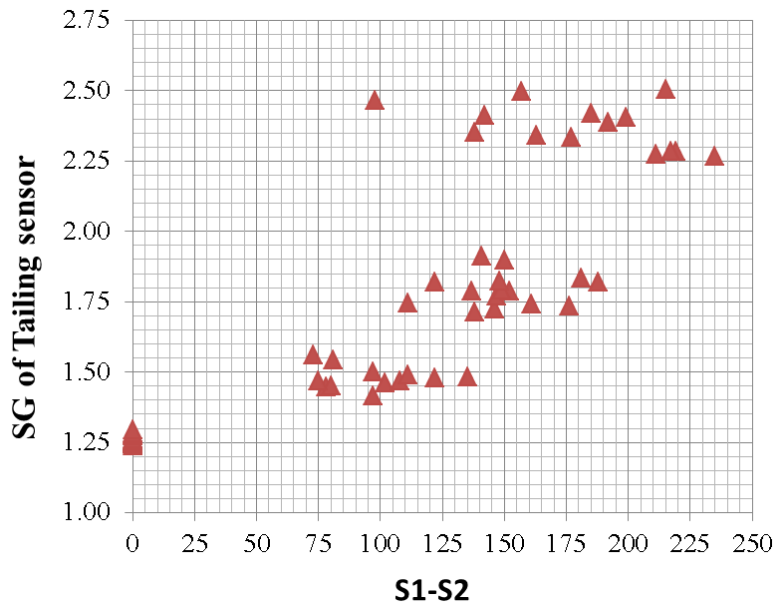

Figure 22: Data variation with increasing tailings SG
(S1: tailings sensor reading, S2: clean coal sensor reading).

In the first phase design, the tailings sensor sample collection point was fixed at the bottom (tailings section) of the spiral trough where tailings SG consistently measured around 2.0 or higher. After learning that higher tailings SG means less accurate sensor readings, it was decided to attach the tailings sensor sample collector to the splitter where the sample density would be much less than tailings sample density at a fixed location near the center of the spiral, and it would be close to the desired density cut point of the spiral as it is always moving with the splitter. This splitter box modification, shown in the Figure 23 schematic, produces a lower tailings SG resulting in greater accuracy in tailings sensor readings.
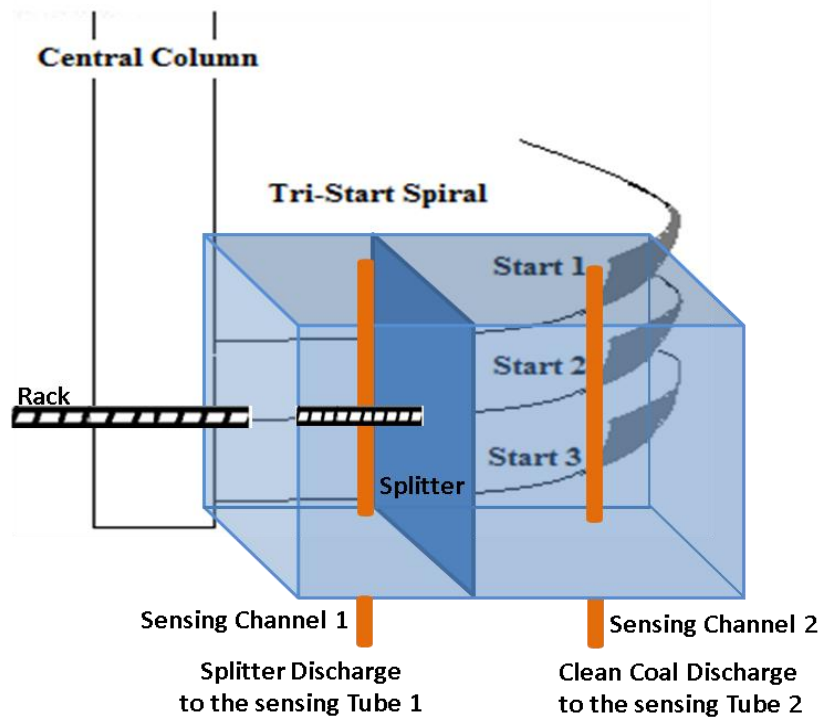
Figure 23: Modified position of tailings sensor sample collector attached to the splitter.

Testing Automation System for Splitter Positioning to Achieve Desired Density Cut Point

After final modifications on the splitter box and finalizing the PCB set up with programs containing the calibration line obtained from calibration testing, the automation system was ready for the real testing. The testing cycle algorithm for adjusting the splitter position is given in Figure 24. After packing the sensor tubes for 180 seconds, the PCB starts reading for 60 seconds and gives the difference between two clean coal and tailings sensor readings. This cycle can be repeated several times and readings averaged for more reliable data. Then, the PCB calculates the tailings SG from the calibration equation and by assuming a linear relationship between SG and the distance from the clean coal sensor. The clean coal sensor sample collector position, which is fixed at the clean coal section of the spiral, was assumed to be the reference point for measuring distances. The splitter could move through a 7-inch span starting at two inches and going to nine inches from the fixed clean coal sampling point toward the tailings section. The position two inches from the fixed clean coal sensor sample collector point was assumed to be the starting point for measuring the position of the splitter.

The initial position for the splitter before starting the automation routine is 3.5 inches from the starting point, i.e., at the midpoint of its range of motion. After activating the automation system, the algorithm shown in Figure 24 begins to run. Table 7 shows recorded outputs illustrating how the automation system adjusts the splitter position for Hawk Eye coal. Negative values in the motor movement column indicate that the splitter is moving toward the clean coal sampling point.
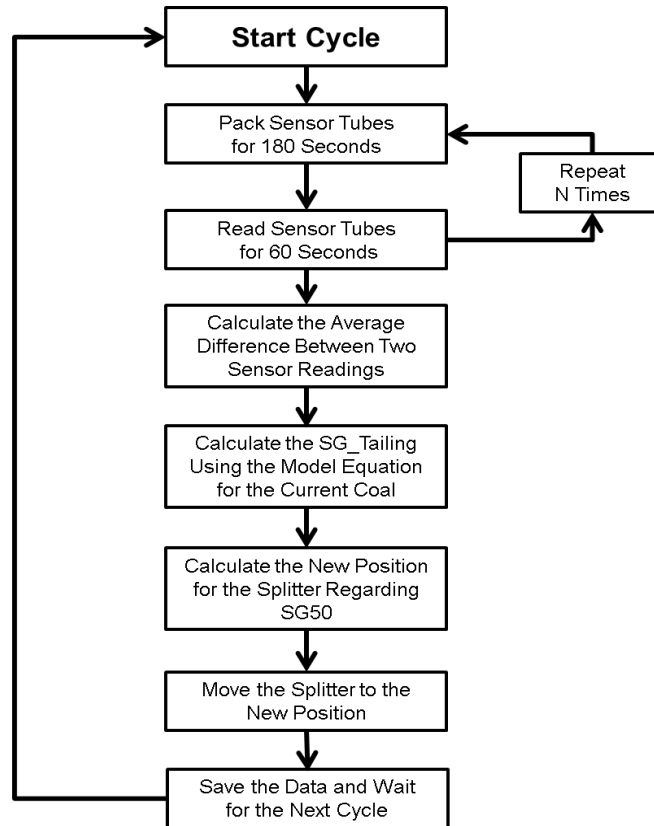
Figure 24: Testing cycle algorithm for adjusting the splitter position.

Table 7: Results from testing spiral automation system with Hawk Eye coal.

Round	Starting Splitter Position (in)	S1 Tailings Sensor Reading (millivolt)	S2 Clean Coal Sensor Reading (millivolt)	S1-S2 (millivolt)	Tailings SG (from calibration equation)	Motor Movement (seconds)	New Splitter Position (in)
1	3.50	305	177	128	1.667	11.7	3.98
2	3.98	310	163	147	1.777	-22.2	3.07
3	3.07	281	157	124	1.646	19.6	3.87
4	3.87	296	163	133	1.694	1.7	3.94
5	3.94	290	161	129	1.672	9.3	4.32
6	4.32	314	148	166	1.908	-24.5	3.32
7	3.32	297	165	132	1.688	4.6	3.51
8	3.51	284	165	119	1.621	24.5	4.75

To limit the influence of sensor tube reading inaccuracies on splitter adjustment, which may be the result of temporary or short-term uncontrollable factors such as the plant shutting down, changes in feed characteristics, or switching coal types, the maximum splitter movement in any round is limited to one inch in either direction. This prevents the automation system from judging the splitter position based on just one round.

Sensor readings from each round shown in Table 8 were checked by collecting samples for SG analysis in the laboratory. Figure 25 is a plot of measured SG values versus SG values predicted by the calibration equation. Once again, it can be seen that as sample density increases, variation in the data also increases. As reported previously, this is because the calibration equation is based on empirical sensor readings which exhibited higher variation as sample SG increased.
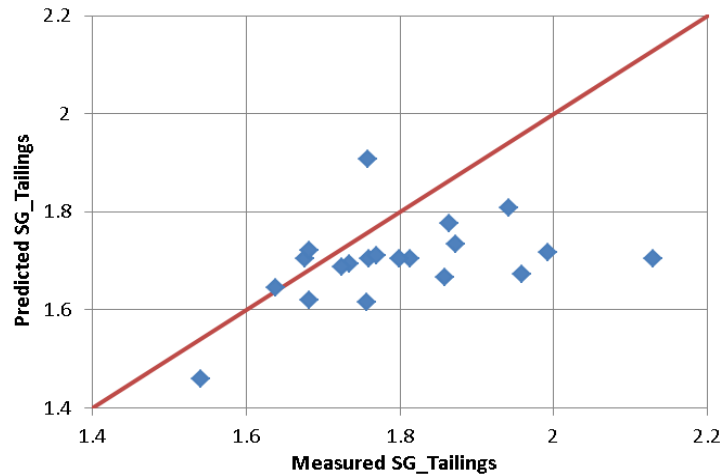

Figure 25: Measured versus predicted tailings SG values.

Task 4: Long-term Testing and Validation of the Spiral Automation System

Fabricating and Installation of a Robust Splitter Box

During initial testing, a number of necessary modifications and adjustments were made to the splitter box, such as attaching the tailings sensor sample collector to the splitter. Thus, prior to long-term testing, a new splitter box incorporating all design changes was fabricated and installed (see Figure 26). It was made out of stronger material for longer life in the plant environment and included improved features for more functionality.

Figure 26: New robust splitter box installed in Creek Paum plant.

Long-term Validation Testing

A series of tests were conducted over a 3-month period to compare smart spiral performance with that of conventional spirals operating in the plant. For each of the 30 tests listed in Table 8, a set of five samples were collected as follows: a common feed sample, product and tailings samples from the smart spiral, and product and tailings samples from a conventional spiral operating in the plant. These samples were analyzed in the laboratory to determine coal cleaning performance data for the +100 mesh size fraction of the feed.

The clean coal yield obtained from both spiral types are compared in Figure 27. In the plant's targeted product ash range of 9-10%, the highest clean coal yields for the conventional spiral varied from 78.0 to 78.9%, whereas the highest clean coal yields of 80.2 to 81.6% for the smart spiral were significantly better.

Combustible recovery values were compared at four different exact ash rejection values, as indicated by arrow marks in Figure 28. At an ash rejection level of 65.7%, combustible recovery for the smart spiral was 91.8% versus 91.3% for the conventional spiral. Similar results at ash rejection levels of 67.3%, 69.7%, and 71.2% were 92.3% versus 89.8%, 93.1% versus 89.9%, and 92.8% versus 92.7%, respectively. Overall, the improvement in clean coal recovery achieved with the smart spiral varied over a wide range from a mere 0.1% to a very high value of 3.2%.

Table 8: Comparative test data from long-term testing of the smart spiral.

| Comparative Long-term Test Id	Spiral Feed Slurry %		Smart Spiral Performance							Conventional Spiral Performance						
			Clean Product (%)		Tailng (%)		Clean Coal Yield %	Combustible Recovery %	Ash Rejection %	Clean Product (%)		Tailng (%)		Clean Coal Yield %	Combustible Recovery %	Ash Rejection %
	Ash	Solid	Ash	Solid	Ash	Solid				Ash	Solid	Ash	Solid			
1	22.57	29.26	9.66	23.61	65.99	47.80	77.08	89.93	67.01	9.89	24.69	68.56	47.80	78.38	91.22	65.66
2	24.26	26.77	10.83	25.22	70.70	44.77	77.58	91.32	65.35	9.75	25.38	68.76	44.77	75.41	89.86	69.70
3	23.90	27.96	10.35	25.25	69.45	42.31	77.06	90.79	66.65	9.46	24.80	66.61	42.31	74.73	88.91	70.41
4	21.73	29.98	9.09	26.65	67.42	44.81	78.32	90.98	67.26	8.72	26.27	64.90	44.81	76.84	89.62	69.17
5	22.61	27.92	8.51	24.93	69.20	47.47	76.77	90.76	71.09	8.10	25.80	65.10	47.47	74.55	88.52	73.29
6	20.18	27.71	11.76	24.16	64.24	45.30	83.96	92.81	51.06	8.41	26.89	62.39	45.30	78.19	89.72	67.41
7	21.27	27.74	8.38	26.38	56.96	44.57	73.46	85.49	71.07	8.60	26.42	57.55	44.57	74.11	86.04	70.06
8	22.69	29.14	9.22	18.62	62.11	39.69	74.54	87.52	69.70	8.26	25.51	60.40	39.69	72.33	85.82	73.66
9	22.85	28.62	9.23	27.03	62.19	46.76	74.28	87.39	70.00	9.51	23.81	61.77	46.76	74.46	87.34	69.03
10	22.42	26.54	9.26	22.97	71.36	45.06	78.81	92.18	67.43	9.52	21.81	66.10	45.06	77.20	90.04	67.21
11	21.43	27.71	9.19	24.74	67.88	47.21	79.14	91.47	66.07	8.56	26.88	65.90	47.21	77.54	90.25	69.05
12	21.56	33.66	9.31	29.58	68.87	47.94	79.43	91.84	65.71	8.96	30.23	66.70	47.94	78.18	90.74	67.51
13	21.22	31.44	8.95	28.73	67.10	46.93	78.90	91.19	66.72	9.07	19.59	64.21	46.93	77.97	89.99	66.66
14	22.40	29.66	8.90	28.48	65.58	46.47	76.19	89.44	69.71	9.40	27.60	65.28	46.47	76.74	89.59	67.78
15	22.44	33.60	8.64	29.09	64.76	47.78	75.41	88.83	70.95	8.78	30.08	63.08	47.78	74.85	88.03	70.70
16	20.04	33.57	8.48	30.89	62.84	47.79	78.74	90.12	66.69	9.24	30.24	60.34	47.79	78.87	89.52	63.61
17	20.14	31.75	9.31	28.86	68.55	47.49	81.71	92.80	62.24	8.83	29.00	64.55	47.49	79.70	90.99	65.06
18	20.64	31.31	9.70	30.86	65.25	48.88	80.30	91.37	62.27	8.86	30.49	66.39	48.88	79.52	91.33	65.88
19	26.78	27.28	10.18	24.00	78.27	43.30	75.63	92.77	71.25	9.41	22.50	72.30	43.30	72.39	89.55	74.56
20	24.19	27.65	10.15	19.29	71.43	46.33	77.08	91.36	67.66	9.89	25.82	71.69	46.33	76.86	91.36	68.58
21	25.28	28.86	10.04	27.98	76.87	48.90	77.19	92.94	69.34	10.18	25.95	75.29	48.90	76.81	92.33	69.06
22	33.12	27.41	11.40	23.38	82.87	49.73	69.61	92.22	76.04	11.28	24.74	80.18	49.73	68.30	90.60	76.75
23	29.33	29.53	10.71	26.66	77.02	49.41	71.92	90.87	73.74	10.98	26.89	76.93	49.41	72.18	90.92	72.97
24	29.71	31.01	10.27	26.54	78.91	51.91	71.68	91.51	75.23	10.54	26.94	78.07	51.91	71.62	91.15	74.59
25	35.19	31.16	11.28	27.21	78.99	51.18	64.70	88.56	79.25	11.11	27.61	76.96	51.18	63.43	87.00	79.98
26	32.09	30.32	10.67	27.98	77.86	48.02	68.12	89.61	77.35	9.97	28.51	74.59	48.02	65.77	87.19	79.57
27	24.49	30.40	9.56	27.97	76.71	47.81	77.78	93.15	69.62	9.16	27.36	75.71	47.81	76.97	92.59	71.20
28	27.22	27.07	10.61	26.53	76.78	46.46	74.89	91.99	70.82	9.47	23.09	72.89	46.46	72.01	89.57	74.96
29	22.60	27.14	9.68	24.02	70.71	45.32	78.83	91.99	66.24	9.42	25.42	68.39	45.32	77.65	90.87	67.63
30	22.36	28.11	8.74	26.08	69.66	44.87	77.64	91.26	69.66	10.19	25.32	66.58	44.87	78.41	90.71	64.27
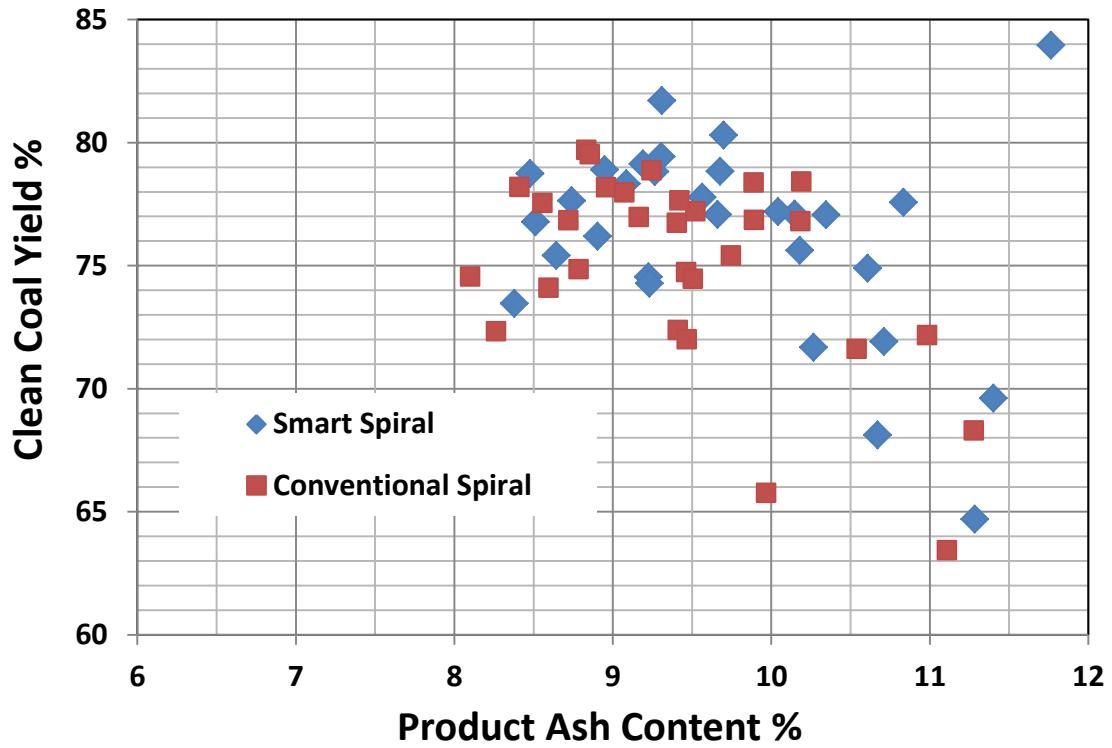
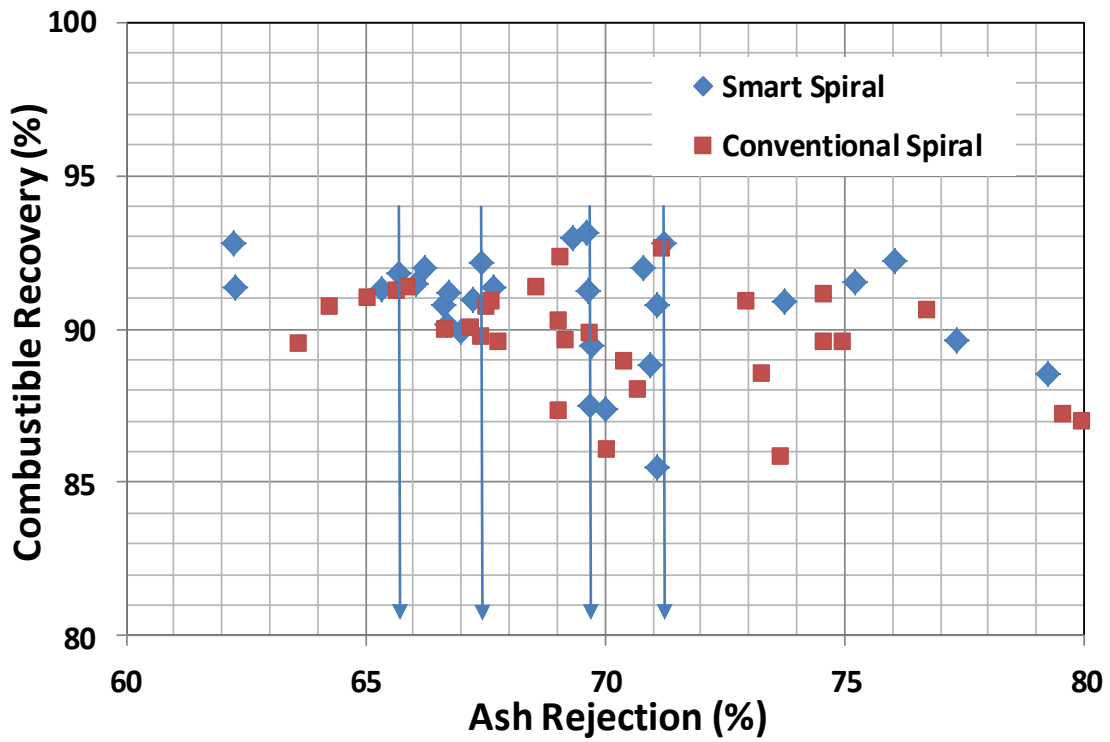Figure 27: Clean coal yield versus ash content.

Figure 28: Combustible recovery versus ash rejection.

Task 5: Open Demonstration

An open demonstration was conducted on June 19, 2013 to inform the coal preparation community in Illinois and beyond about the new spiral automation system developed in this project. Nearly thirty professionals attended the event.   These included representatives from a variety of coal companies including Illinois operators Alliance Coal, Foresight Energy, and Knight Hawk Coal. Coal-fired power generation companies such as Southern Illinois Power Cooperative, as well as equipment manufacturers including PrepTech/Multotec, Birtley, and NDT were also represented. Government agencies represented included the ICCI and the Office of Coal Development of Illinois' Department of Commerce and Economic Opportunity. The demonstration was reported on the local television station, WSIL-TV, during their evening newscasts. A few photographs of the demonstration are provided in Figure 29.

Figure 29: Open demo held at the Creek Paum preparation plant site on June 19, 2013.

Task 6: Economic Analysis

The SSSC consists of three major components, namely the splitter box assembly, the sensor tube assembly, and the control system assembly. The latter includes the PCB assembly. Known fabrication costs for each of these components were significantly higher for this project than they would be for a commercial installation due to the prototype nature of components in a research project. Nevertheless, estimated costs for large-scale commercial production are as follows:

Sensor Tubes, DC motor, and splitter box assembly: $150
PCB components (IC components and connectors): $150
PCB fabrication: $80
PCB assembly: $70

Thus, the SSSC is expected to add an additional cost of $450 to a set of triple-start spirals capable of processing nearly 10 tph of raw coal. Long-term test results indicate that the smart spiral may provide about 2% more clean coal yield, or 0.2 tph of clean coal. This would produce an additional 800 to 1,500 tons per year of clean coal generating $40,000 to $75,000 in added revenue for each triple-start spiral. Clearly, a commercial spiral automation system has a very short payback period justifying efforts leading to rapid commercialization of the technology.

CONCLUSIONS AND RECOMMENDATIONS

- The spiral automation system, named SIU's Smart Spiral Component (SSSC), consisting of a splitter box assembly, electrical conductivity-based sensor tubes, and a control system assembly, was successfully developed and demonstrated to the Illinois coal preparation community in an operating coal preparation plant.
- A comparative series of tests conducted over a 3-month period showed that the clean coal yield obtained for the smart spiral was 2.2 to 2.7 percentage points higher than that of the conventional spiral operating in the plant in the desired product ash range of 9 to 10%. This performance improvement resulted from an increase in combustible recovery of about 3% at an ash rejection level of nearly 70%.
- Adding the spiral automation system to a set of triple-start spirals is expected to add an additional cost of $450. For a set of triple-start spirals capable of handling nearly 10 tons per hour of raw coal, the spiral automation system is expected to increase clean coal yield by 2% resulting in 0.2 tph or 800 to 1,500 tons per year of additional salable product. That amounts to $40,000 to $75,000 of added revenue generated by each triple-start spiral.
- The economic analysis clearly indicates that the spiral automation system has great commercialization potential; however, cost estimates for the SSSC are based on single unit installations and not mass production levels.
- The spiral automation system has only operated at a commercial level on a single triple-start spiral. Scale up to multiple units operating simultaneously is essential to demonstrating the commercialization potential of the technology.

ACKNOWLEDGEMENTS

REFERENCES

Abbott, J., 1982. "The Optimization of Process Parameters to Maximize the Profitability from a Three-Component Blend." Proceedings of 1st Australian Coal Preparation Conference, April 6-10, Newcastle, Australia, pp. 87-105.

Kim, L-H., N-K. Hahm, W-C. Lee, J-S. Yu, Y-C. Kim, C-Y. Won, and Y-R. Kim, 2006. "Analysis of a New PWM Method for Conducted EMI Reduction in a Field Oriented Controlled Induction Motor." Proceedings of 21st IEEE Applied Power Electronics Conference and Exposition, March 19-23, Dallas, TX, pp.204-210.

Luttrell, G.H.; R.Q. Honaker, and F.L. Stanley, 2003. "Operating Guidelines for Coal Spiral Circuits." Proceedings of 20th International Coal Preparation Exhibition and Conference, April 29-May 1, Lexington, KY, pp. 69-78.

Mohanty, M.K., 2007. "Automation and Performance Improvement of Spiral Concentrators." Final Technical Report for ICCI Project No. 06-1/2.1A-6.

Mohanty, M.K., 2011. "Development and Demonstration of an Automation and Control System for Coal Spirals." Final Technical Report for ICCI Project No. 10/4B-4.

Muttaqui, K.M. and M.E. Haque, 2008. "Electromagnetic Interference Generated from Fast Switching Power Electronic Devices." *International Journal of Innovations in Energy Systems and Power*, Vol. 3, No. 1, April, pp. 19-26.

DISCLAIMER STATEMENT